Microstructure characterization of meat by quantitative MRI

Jean-Louis Damez, Sylvie Clerjon, Roland R. Labas, Jeanne Danon, Frederic Peyrin, J.-M. Bonny

MICROSTRUCTURE CHARACTERIZATION OF MEAT BY QUANTITATIVE MRI

J.L. Damez, S. Clerjon, R. Labas, J. Danon, F. Peyrin and J.M. Bonny

INRA, UR370 Qualité des Produits Animaux, F-63122 Saint Gènes Champanelle, France.

Abstract – Characterizing the behavior of water diffusion within a volume element (voxel) provides a means for describing inner microstructure at a cellular scale, taking into account experimental diffusion times and apparent diffusion coefficients measured in muscle. The mean square displacement of water molecules is close to the dimensions of cells of the order of microns. As muscle, and meat, is highly organized in a fibrillar structure, the diffusion of water is facilitated in the fiber direction. We therefore modeled this anisotropic diffusion voxelwise using ellipsoid by means of a first order tensor, according to Diffusion Tensor Imaging (DTI). We also applied this modeling at different degrees of diffusion sensitization (given by the b-value). New diffusion parametric maps were obtained on tissue that have been registered with high-resolution anatomical images obtained by MRI and histology to put in obvious relationships between meat microstucture and diffusion parameter observed at a meso-scale. Diffusion decays were measured at a mesoscopic scale. From these data, first order tensor fitting at each b-value, and subsequent diagonalisation revealed a diffusion reference frame in an anisotropic medium. Maps of diffusion parameters (e.g. eigenvalues or trace of the diffusion tensor, diffusion anisotropy, difference between mono and multi-exponential fits) were superimposed on anatomical images, i.e. histological and high-resolution susceptibility-weighted MR images (SWI), revealing structural details which do not appear in SWI.

Key Words – magnetic resonance imaging, meat structure, water diffusion

I. INTRODUCTION

Molecular diffusion in cellular tissues differs from diffusion in free solutions because compartments made by fibers hinder and/or restrict Brownian motion. Both size and shape as well as interactions within the different compartments can influence the diffusion properties. By quantitative magnetic resonance imaging (qMRI), a physico-chemical parameter could be mapped in voxel. It then may become possible to "see" structural architecture, not directly and destructively as done by tomography microimaging, but indirectly and non-destructively by using diffusion qMRI.

Even if diffusion qMRI is a generic method to assess Brownian random motion of molecules, it was mostly applied to water which is abundant in biological tissues and visible by MRI.

Free or restricted diffusion?

Accurate modeling of water diffusion process in biological tissues should first consider free or restricted diffusion:

Free diffusion

When water molecules obey a free Gaussian diffusion, the diffusion weighted signal S follows a monoexponential decay as function of the diffusion sensitization factor *b* [1]:

$S(b)=Sa \exp(-b.\ A)$,

where A is the apparent diffusion coefficient.

Restricted diffusion

When restricted diffusion is considered due to obstacles (e.g. proteins, cells), a (empirical) bi-exponential decay law should be used [2]:

$S(b)=Sa \exp(-b.A)+Sb \exp(-b.B)$

Isotropic or anisotropic diffusion?

Apparent diffusion coefficient can also change with direction because of the presence of organized structures.

For example in a group of fibers having the same direction, the apparent diffusion coefficient is:

- maximum in the fibre direction
- minimum orthogonally to the fibre direction.

If the structure is anisotropic, as in muscle [3], water diffusivity also displays anisotropic behavior.

If water movements are vectorized, water diffusion is expressed by tensors. A first-order tensor fits the diffusion anisotropy with an ellipsoid [4]. Such a model suffices for most of muscles, because most often there are no crossing fascicles at the scale of the voxel. Therefore the diffusion weighted signal can be expressed in the case of free diffusion by

$$S(b)=Sa \exp(-b.\ |A|) \qquad |A|=\begin{vmatrix} a_{11} & a_{12} & a_{13} \\ a_{21} & a_{22} & a_{23} \\ a_{31} & a_{32} & a_{33} \end{vmatrix}$$

where the tensor |A| replaces the previous isotropic apparent diffusion coefficient.
As a result, the following model is relevant when considering both restricted and anisotropic diffusion:
$S(b) = Sa \exp(-b.|A|) + Sb \exp(-b.|B|)$
Our objective is to obtain **high resolution imaging of meat tissue microstructure in situ by MRI** using diffusion tensor imaging (DTI) at different *b*-values in order to assess by quantitative imaging the fibrillar structure of muscle tissue at the mesoscopic scale (using our quantitative model of water diffusivity which is linked to the tissue structure).

II. MATERIALS AND METHODS

Diffusion gradients were applied in six non-collinear and bi-orthogonal directions required for diffusion tensor imaging (DTI). The goal is to construct a fiber orientated frame in each voxel of the meat tissue sample. Regardless of the sample orientation relative to the magnet, diffusion weighted signals were obtained with gradient fields applied in 6 directions (Figure 1) and then calculation (tensor diagonalization) was made in order to consider diffusion in the fiber oriented frame. The huge advantage of this approach is that the diffusion (closely linked to the spatial fiber organization) is then assessed free of the effects of local fibers orientations.

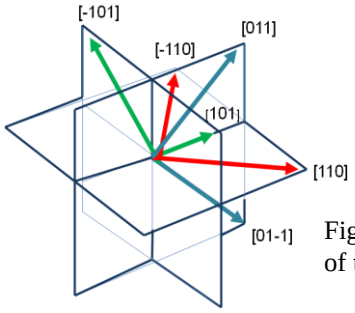

Figure 1. The 6 directions of the gradient vectors

After diagonalization, the first eigenvector, which is constant for all the *b*-values, corresponds to the main fiber axis direction. The second and third eigenvectors where also quite similar and correspond to the 2 orthogonal directions of the fiber axis. Other elements (not eigenvectors) are residues (local dispersion of fiber direction within a voxel). The tensor being symmetrical, only 6 terms differ which are shown as maps in Figure 2. The same process was applied to each 6-directions dataset at increasing *b*-values (ranging 100-20000 s/mm²) (Figure 3).

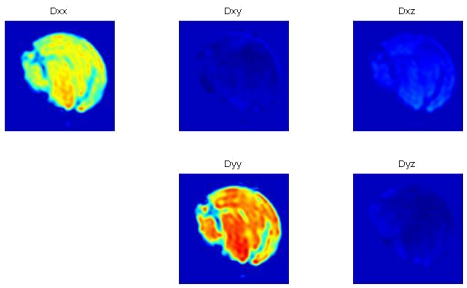

Figure 2. Diffusivities (respectively Dxx, Dyy and Dzz) along x, y and z axes (xx, yy, zz eigenvalues direction) and cross-terms obtained by DTI for a given *b* value (*b*= 2000 s/mm^2)

Figure 3. DT maps derived from the 240 diffusion weighted images were acquired consisting in:
- 6 non-collinear directions
- 40 b-values ranging 100-20000 s/mm2

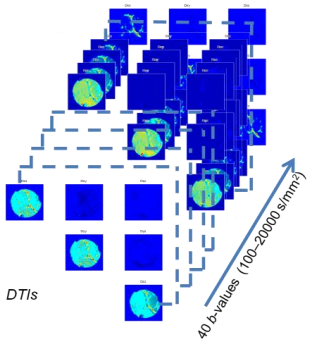

Because of the constant direction of the first eigenvector with *b*-value, diffusion behavior was decomposed voxelwise into two decays, (Dxx) and (Dyy + Dzz)/2 corresponding respectively to a direction parallel and perpendicular to the local fiber direction.
Diffusion decays were measured at a mesoscopic scale (30 × 30 matrix of .5 mm × .5 mm × .5 mm voxels). In order to register diffusion maps and histological images, 5 contiguous MR images showing intra-muscular anatomical details (5 contiguous .5 mm spaced 300x300 matrix of .05 mm × .05 mm × .25 mm voxels) were also took on each meat sample. Experiments were conducted at 400 MHz on fresh meat (pork *biceps femoris* and *maceter* samples Ø = 15 mm) at 8°C. Total acquisition time for one sample took approximately 18 H. All mathematical treatments and computations were performed using Matlab software.

III. RESULTS AND DISCUSSION

Each pixel of the resulting quantitative maps corresponds to a group of orientated fibers. If we consider the same voxel, or a group of voxels, one can examine on different parameters, such as

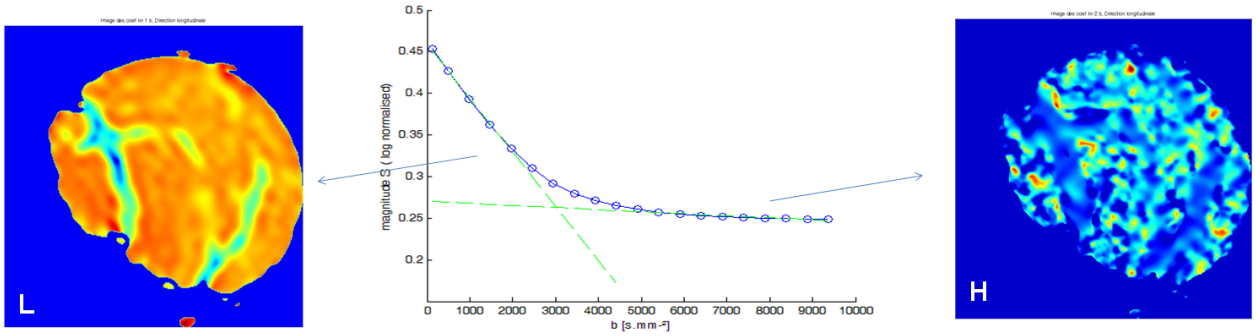

Figure 4. Diffusion-weighted intensity attenuation exhibiting hindered and restricted diffusion from the trace of the diffusion tensor matrix. L image (left) is at low *b* value that inhibits high diffusion corresponding to hindered diffusion , H image (right) is at high *b* value that inhibits low diffusion corresponding to restricted diffusion.

diffusion anisotropy, difference between mono and multi-exponential fits.

For example, diffusion anisotropy can be assessed by the ratio between the first eigenvalue map with the mean of the second and third eigenvalue maps. Also, after bi-exponential fitting of the two // and ⊥ decays, one can map the relative amplitudes of the two exponentials.

Quantitative mapping

// and ⊥ decays both deviate from the Gaussian diffusion, expressed by a mono-exponential decay since they follow a bi-exponential shape (Figure 4). This highlights hindered and/or restricted diffusion of water, out of and into muscle fibers, or exchanging between the two compartments.

Diffusion maps reveal details due to spatial variations of structure at a resolution much below the acquisition resolution.

Identification of structural and morphologic components

After spatial registration, histological images were superimposed on high-resolution susceptibility-weighted gradient-echo images (SWI, with 300 × 300 matrix of voxels) to identify morphologic components (fat/collagen network), and subsequently superimposed on quantitative diffusion maps (Figure 5).

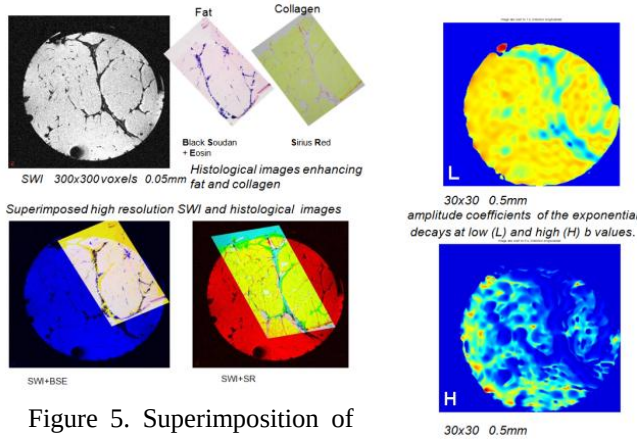

Figure 5. Superimposition of histological and diffusion

Relationship between diffusion and muscle fibers types

To assess the architecture of the muscle, we investigated into the relationship between diffusion and muscle fibers types. Histological cuts (approximatly1mm x1mm) were observed after histoenzymological ATPase staining with pH 4.35 preincubation. These histological images were superimposed to SWI and subsequently to quantitative diffusion maps.

At low *b*-values, diffusion parameters seem to correlate with metabolic characteristics of meat fibers, as highlighted by photomicrography of areas characterized by histoenzymological ATPase staining (Figure 6).

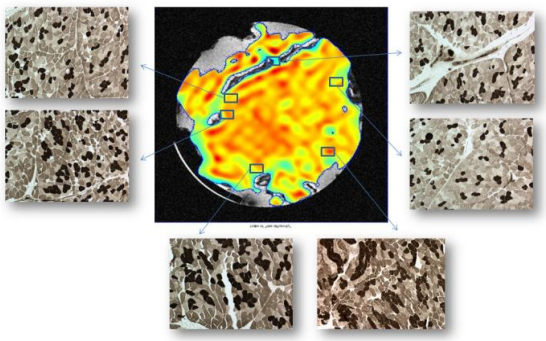

Figure 6. Superimposition of histoenzymological ATPase stained and diffusion image

On the histoenzymological images the three intensities are black (type I), white (IIA) and grey (IIX plus IIB). Diffusion is mapped with a blue/green to orange/red scale. Type I fibers (blacks) seem correlate with regions of high diffusivities as type II fibers (greys and whites) with regions of low diffusivities. A quantitative analysis between

diffusivities and the areas occupied by the different fiber types deserves further study

Variability of the dimensions of structural components

Structure of muscle is strongly organized in set of fiber bundles more or less aligned depending on type and functionality of the muscle. The muscle structure can be roughly modeled as a square lattice arrangement of fluid-filled cylinders surrounded by fluid. The signal attenuation dependence within this simple cylinder geometry has been analytically described elsewhere [5, 6] versus *q*-value instead of *b*-values (where the reciprocal wave number $q = \gamma g \delta / 2\pi$ with γ giromagnetic ratio, δ diffusion gradient duration, g diffusion gradient amplitude). The theorical diffusion decay plot exhibits deep gaps in attenuation curves that have been directly correlated to the geometry of the cylinder lattice. We have attempted to determine if such attenuation behavior can be found in the real meat structure made of aligned fibers.

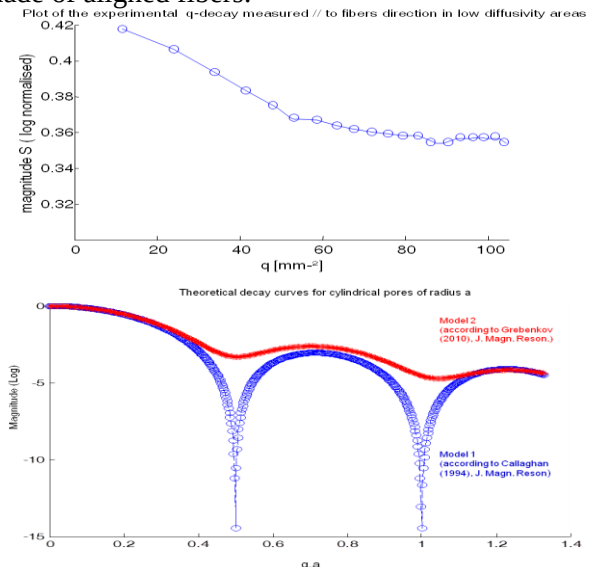

Figure 7. Echo decay attenuation observed on localized area compared to 2 different prediction models

Several minima in the echo decay vs *q* can be observed on models where meat fiber bundles are assumed to be a simple oriented geometry of an array of water filled impermeable tubes of ϕ 50µm (Figure 7). However less deep minima amplitudes on acquired data in homogeneous region are observed compared to the prediction of models. The experimental data plot deviates from the theoretical plot mainly due to the heterogeneity in the fibres diameter and also perhaps the non strictly impermeability of the fibres membranes. To the best of our knowledge, it is the first time that such scatter-like behavior was observed in a biological matrix which seems very promising for quantifying structural information from the resulting diffusion attenuation plots.

IV. CONCLUSION

We have showed that characterizing the behavior of water diffusion within a voxel provides a means for describing the inner microstructure at a cellular scale, taking into account apparent diffusion coefficients measured in muscle. Using the anisotropy of water diffusion due to the highly fibrillar structure of meat, we modeled this diffusion in three dimensions using tensors. We used Diffusion Tensor Imaging (DTI) with different *b*-values to obtain high resolution diffusion parameter mapping of tissue which were registered to high-resolution susceptibility-weighted gradient-echo images and histological images to determine if there existed relationships between meat microstucture and diffusion observed at a meso-scale. Promising results have been obtained showing structural details correlated with metabolic characteristics. Future efforts will be put on the differentiation within type of meat muscle and meat fibers types and on the variability of the structural components.

ACKNOWLEDGEMENTS

This study was conducted under the umbrella of the European DREAM project. The MRI experiments were performed at the biological systems MR platform at the INRA Center of Clermont-Ferrand, France (www.clermont.inra.fr/rmsb/).

REFERENCES

1. H. C. Torrey (1956) Bloch Equations with Diffusion Terms Phys. Rev., 104: 563–565
2. M.L. Milne, M.S. Conradi (2009) Multi-exponential signal decay from diffusion in a single compartment J. Magn. Reson., 197 (1): 87-90
3. G.G. Cleveland, D.C. Chang, C.F. Hazlewood, H.E Rorschach (1976). Biophys. J., 16 (9): 1043-1053
4. P.J. Basser, J. Mattiello, D. Le Bihan (1994) MR diffusion tensor spectroscopy and imaging. Biophys. J., 66:259-267
5. D. S. Grebenkov (2010) Pulsed-gradient spin-echo monitoring of restricted diffusion in multilay structures. J. Magn. Reson., 205: 181–195
6. P.T. Callaghan (1995) Pulsed gradient spin echo NMR for planar, cylindrical and spherical pores under conditions of wall relaxation. J. Magn. Reson., A, 113: 53–59